Some Trim Drag Considerations for Maneuvering Aircraft

LINWOOD W. MCKINNEY* AND SAMUEL M. DOLLYHIGH†
NASA Langley Research Center, Hampton, Va.

The results of a preliminary analytical and experimental study of trim drag characteristics at maneuvering lift coefficients have been summarized. The study included aft-tail configurations at subsonic and supersonic speeds and canard configurations at subsonic speeds. It is shown that the tail load required to minimize trim drag is highly dependent on the wing-body drag-due-to-lift characteristics with examples presented for both the full and zero leading-edge suction cases. For the high drag case (corresponding to zero leading-edge suction), which tends to be typical at high maneuvering lift coefficients and high speeds, rather large uploads on the tail are required to reduce the trim drag problem. The analytical predictions of trim drag characteristics compare well with the experiment for the aft-tail configuration. At supersonic speeds, reductions in down tail load required to trim, obtained by increasing tail volume and thereby allowing a favorable rebalancing of the aircraft, result in relatively large reductions in trim drag for aft-tail configurations. At subsonic speeds, the experimental studies for the canard configuration exhibit considerably higher trim drag than the analytical prediction as a result of canard stall.

Nomenclature‡

ac	= aerodynamic center
$\bar{c}$	= wing mean aerodynamic chord
C_D	= total drag coefficient
C_{D_0}	= drag coefficient at zero angle of attack
$\Delta C_{D_{\text{trim}}}$	= trim drag increment (drag increment between wing-body drag curve and trimmed drag curve at a constant lift coefficient)
C_L	= lift coefficient, based on wing area
C_{L_0}	= lift coefficient at zero angle of attack
$\Delta C_{L_{\text{tail}}}$	= increment in total lift coefficient carried on the horizontal tail
$C_{L_{it}}$	= lift coefficient due to deflection of horizontal tail, per deg
C_{L_α}	= slope of lift curve with angle of attack, per deg
C_m	= pitching-moment coefficient
C_{m_0}	= pitching-moment coefficient at zero angle of attack
$C_{m_{it}}$	= pitching moment due to deflection of horizontal tail at constant α, per deg
C_{m_α}	= slope of pitching-moment curve with angle of attack, per deg
i_t	= slope of pitching-moment curve with angle of attack, per deg
i_t	= incidence angle of horizontal tail, deg
l_t	= horizontal-tail arm, distance from center of gravity to center of pressure on horizontal tail, ft
M	= Mach number
q_0	= freestream dynamic pressure, lb/ft^2
q_t	= local dynamic pressure at the horizontal tail, lb/ft^2
S_t	= reference area of horizontal tail
S_w	= reference area of wing
V_t	= tail volume coefficient, $l_t S_t/\bar{c}S_w$
α	= angle of attack, deg
δ_c	= angle of deflection of canard, deg
ϵ	= downwash angle, deg
ϵ_0	= downwash angle at zero angle of attack, deg
$\partial C_D/\partial C_L{}^2$	= drag-due-to-lift factor, variation of drag coefficient with lift coefficient squared
$\partial\epsilon/\partial\alpha$	= variation of downwash with angle of attack

Subscripts

t	= refers to horizontal tail
w	= refers to wing body
trim	= refers to trimmed conditions

Presented as Paper 70-932 at the AIAA 2nd Aircraft Design and Operations Meeting, Los Angeles, Calif., July 20–22, 1970; submitted September 23, 1970; revision received January 15, 1971.

* Aerospace Technologist. Member AIAA.
† Aerospace Technologist. Associate Member AIAA.

‡ Primed quantities are nondimensionalized with respect to tail area and chord.

Introduction

TRIM drag has been the subject of a number of papers published in the past[1,2] and probably the most widely known of these is the paper by Graham and Ryan.[1] In these analyses, however, the emphasis was primarily on 1-g flight and supersonic speeds. The present analysis is concerned with the maneuvering case and emphasizes the subsonic speed range.

In view of the many variables involved in an analysis of trim drag and the interaction with stability and control characteristics, it was considered desirable to supplement the analytical study with a wind-tunnel investigation of a general research model that could be used to study both aft-tail and canard configurations.

Figure 1a shows a sketch of the model in the aft-tail configuration and Fig. 1b shows a sketch of the model in the canard configuration. The model in the canard configuration was designed to utilize two balances: one balance is in the forward fuselage to measure the combined forces and moments of the canard and forward fuselage as indicated by the shaded area of Fig. 1b, and the other in the aft fuselage to measure the total forces and moments on the model. A list of planform and configuration variables that will be studied in the continuing investigation is shown in Table 1. At the present time, however, only limited experimental data have been obtained.

The purpose of the present paper is to summarize some of the preliminary analytical studies that were used as a basis for setting up the research program. These studies will be compared with the experimental results, where available. For aft-tail configurations, the discussion will be concerned primarily with the effects of wing drag due to lift on trim drag at subsonic speeds with a comparison of calculated and experimental trim drag characteristics. The effect of tail volume at supersonic speeds will also be discussed. The adequacy of existing subsonic theory to predict interference effects for canard configurations will be shown, and some

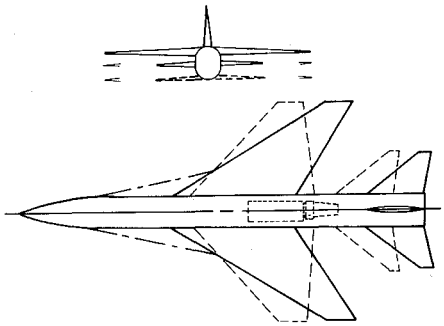

Fig. 1a Sketch of general research model: aft-tail configuration.

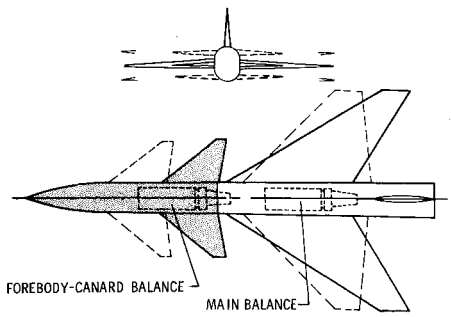

Fig. 1b Sketch of general research model: canard configuration.

comparisons of calculated and experimental trim drag for canard configurations will be discussed.

Method of Analysis

Various definitions of trim drag have been employed over the years and the one selected for use in this paper is illustrated in Fig. 2. The total trimmed drag polar is separated, for analysis considerations, into the drag of the wing body and the trim drag associated with trimming the wing-body moments. The trim drag increment listed on Fig. 2 as $\Delta C_{D_{\text{trim}}}$ is composed of an increment in drag on the wing due to the change in wing lift coefficients required to offset the tail load and the drag associated with the tail. It should be noted that Fig. 2 represents trimming with a down load on the tail.

In this study, the aerodynamic characteristics of the component parts of the airplane were obtained from lifting surface theories (Ref. 3 for subsonic and Ref. 4 for supersonic), and used as input to the following equations to calculate the trim drag $\Delta C_{D_{\text{trim}}}$ as a function of tail load. The lift and drag of the tail referenced to the local velocity at the tail are

$$\Delta C_{L_t} = \{C_{L_{i_t}}' i_t + C_{L_{\alpha_t}}'[-\epsilon_0 + (1 - \partial\epsilon/\partial\alpha)\alpha] + C_{L_{0_t}}'\} S_t/S_w \cdot q_t/q_0 \quad (1)$$

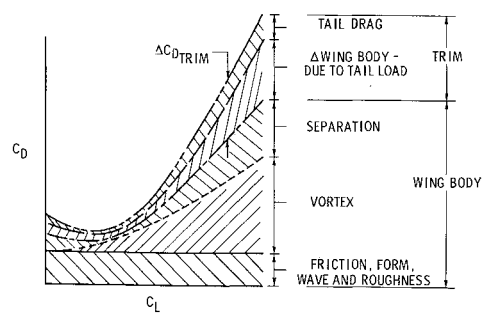

Fig. 2 Definition of trim drag.

Table 1 Planform and configuration variables for research model

Item	Aft-tail configuration Variations
Wing	Camber, warp, section, sweep, location, planform, and leading- and trailing-edge flaps for maneuvering
Horizontal tail	Size, location (vertical and horizontal)
Item	**Canard configuration Variations**
Wing	Camber, warp, section, sweep, location, and leading- and trailing-edge flaps for maneuvering
Canard	Size, planform, location (vertical and horizontal) and trailing-edge flaps for control

$$\Delta C_{D_t} = (\partial C_D/\partial C_L^2)_t'\{C_{L_{i_t}}' i_t + C_{L_{\alpha_t}}'[-\epsilon_0 + (1 - \partial\epsilon/\partial\alpha)\cdot\alpha] + C_{L_{0_t}}'\}^2 S_t/S_w \cdot q_t/q_0 \quad (2)$$

where

$$i_t = i_{t_{\text{trim}}} = -\{C_{m_{0_w}} + C_{m\alpha_w}\cdot\alpha + C_{L\alpha_t}'[-\epsilon_0 + (1 - \partial\epsilon/\partial\alpha)\alpha] l_t/\bar{c}_w \cdot S_t/S_w \cdot q_t/q_0\}/C_{L_{i_t}}' \cdot l_t/\bar{c}_w \cdot S_t/S_w \cdot q_t/q_0 \quad (3)$$

The total trimmed lift and drag are

$$C_{L_{\text{trimmed}}} = C_{L_{0_w}} + C_{L\alpha_w}\cdot\alpha + \Delta C_{L_t}\cos\epsilon - \Delta C_{D_t}\sin\epsilon \quad (4)$$

$$C_{D_{\text{trimmed}}} = C_{D_{0_w}} + C_{D_{0_t}} + (\partial C_D \partial C_L^2)_w (C_{L_{0_w}} + C_{L\alpha_w}\cdot\alpha)^2 + \Delta C_{D_t}\cos\epsilon + \Delta C_{L_t}\sin\epsilon \quad (5)$$

where

$$\epsilon = \epsilon_0 + \partial\epsilon/\partial\alpha\cdot\alpha \quad (6)$$

The tail load referenced to wing area is

$$\Delta C_{L_{\text{tail}}} = \Delta C_{L_t}\cos\epsilon - \Delta C_{D_t}\sin\epsilon \quad (7)$$

and the trim drag at a constant total lift coefficient is

$$\Delta C_{D_{\text{trim}}} = C_{D_{\text{trimmed}}} - [(C_{D_{0_w}} + C_{D_{0_t}}) + (\partial C_D/\partial C_L^2)_w \times (C_{L_{0_w}} + C_{L\alpha_w}\cdot\alpha_{\text{trim}})^2] \quad (8)$$

These equations, although written in terminology for an aft-tail configuration, are also applicable for canard configurations when the canard aerodynamic and physical characteristics are substituted for the tail terms and the downwash is set equal to zero. Since the downwash terms apply to the wing in the case of canard configurations, it is more appropriate to obtain these effects from a lifting-surface theory that accounts for mutual interference between the wing and canard. In this case, the vortex lattice lifting-surface theory of Ref. 3 was used.

In the present analysis, the drag-due-to-lift parameter of the wing and tail/canard were considered separately rather than integrating the total span load of the airplane. At the high-lift coefficients of concern for maneuvering aircraft where near-zero leading-edge suction usually exists on the wing, this is not believed to result in significant error for aft-tail configurations. For canard configurations where the span load of the wing is significantly altered by downwash from the canard, the absolute drag levels obtained with this simplification may be somewhat in error and further work is required to determine the magnitude. However, it is believed that the trends predicted are valid for preliminary design work.

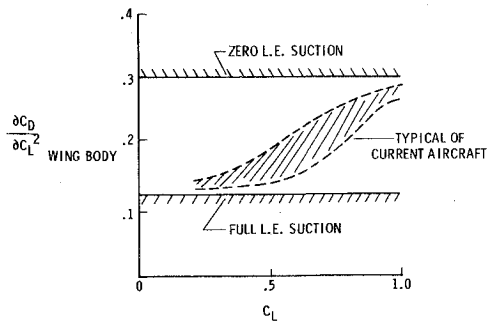

Fig. 3 Typical variation of drag-due-to-lift parameter; aspect ratio = 2.5; subsonic speeds.

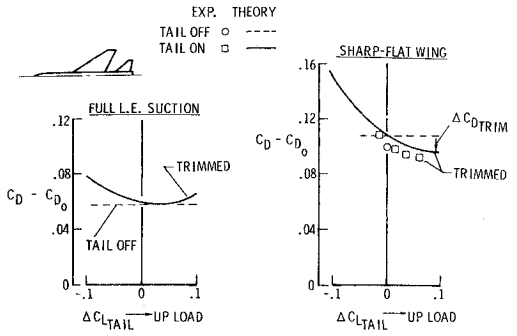

Fig. 4 Effect of wing-body drag-due-to-lift on subsonic trim drag for aft-tail configurations; $M = 0.70$; $C_L = 0.60$.

Importance of Wing Efficiency

One of the more important considerations in a study of trim drag is the efficiency with which the wing operates. Therefore, a typical variation of the subsonic drag-due-to-lift parameter (which is a measure of wing efficiency) is presented in Fig. 3. The full leading-edge suction line and the zero leading-edge suction line are shown for reference. The variation of leading-edge suction with Reynolds number and wing geometry is discussed in a paper by Henderson.[5] The cross-hatched area indicates a typical range of values of the drag-due-to-lift parameter for current aircraft including the use of both fixed camber and twist or wing flaps for maneuvering. At low-lift coefficients ($C_L \approx 0.30$) typical of 1-g flight, drag-due-to-lift values approaching those corresponding to full leading-edge suction are generally obtained. At the high-lift coefficients ($C_L \approx 1.0$) which correspond to the maneuvering case and consequently are of interest in this paper, the drag-due-to-lift typically approaches the zero leading-edge suction line even when current maneuver flap concepts are considered. The need for improving drag-due-to-lift characteristics of wings at the high-lift coefficients by means such as wing warp, improved maneuver devices, and so forth, is recognized and is included in the over-all general research study outlined in Table 1. Wing efficiency is also important at supersonic speeds and must be carefully considered in optimizing maneuvering performance. For this paper, however, the discussion of drag due to lift will be limited to the effects of the full and zero leading-edge suction cases on trim drag.

Aft-Tail Configurations

Subsonic Case

To illustrate the effects of wing-body drag due to lift on trim drag, the calculated variation of trimmed drag with tail load required to trim is presented in Fig. 4 for both the full leading-edge suction and zero leading-edge suction case. The increment between the tail-off and trimmed curve represents the trim drag ($\Delta C_{D_{trim}}$). These calculations were made at a lift coefficient of 0.6 and Mach number of 0.7 in order to obtain a comparison with experimental data from a sharp-flat wing model. The trends predicted, however, are applicable over the lift coefficient range for the two leading-edge suction conditions.

With full leading-edge suction, trimming with a slight upload results in minimum trim drag. The case presented is for a configuration with a low tail (from stability considerations) and, consequently, low downwash ($\partial\epsilon/\partial\alpha = 0.40$). If the tail is placed in a region of higher downwash, the bucket in the trimmed curve will tend to shift to the down tail load side of the figure due to the thrust component obtained from the tail lift vector in the downwash field; since, at subsonic speeds where Mach effects are not large, the increase in drag due to lift on the wing for the full suction case resulting from a down tail load may be offset by the forward inclination of the tail lift vector in a region of high downwash. It is generally desirable, therefore, to trim with a near-zero tail load for wings having full leading-edge suction.

For wings with near-zero leading-edge suction, significant reductions in trimmed drag due to lift can be obtained if the configuration is trimmed with a rather large upload on the tail, which results in a reduction in angle of attack and unloads the wing. With zero leading-edge suction, the increase in wing drag due to a down tail load far exceeds the beneficial effects of the downwash field and the wing contribution is the major portion of the total trim drag. It should also be noted that the benefits shown for trimming with an up tail load at $C_L = 0.6$ would be even greater at a $C_L = 1.0$ due to the increase in wing drag due to lift.

The comparison of the calculations with experimental data for the sharp-flat wing shows good agreement in the trend with tail load. The difference in drag level shown results from a difference between the experimental and the calculated wing-body drag due to lift and is equivalent to an effective leading-edge suction of about 10%.

It is important to remember that although trimming with an upload on the tail at a high-lift coefficient results in trim drag benefits for wings with near-zero leading-edge suction, the total trimmed drag for these wings is much higher than would be the case if full leading-edge suction could be maintained at the high-lift coefficients and Mach numbers of interest for maneuvering.

Significant benefits in subsonic trim drag at the high lift coefficients can be obtained by trimming the aircraft with a relatively large upload on the tail for the state of the art of wing-body drag-due-to-lift characteristics indicated in Fig. 3. As improvements in wing-body drag due to lift are made through further research, the benefits of trimming with an up tail load will become less significant, but at the present state-of-the-art, the wing tail relationship for maneuvering aircraft should receive careful attention.

Supersonic Case

At supersonic speeds, the trim drag problem is further aggravated. A typical comparison of trim drag character-

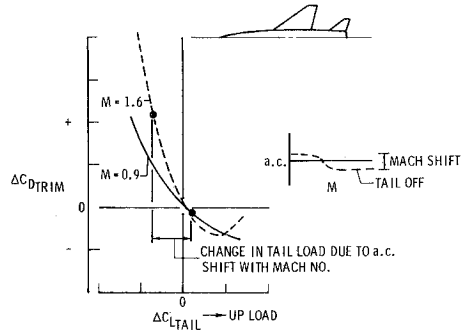

Fig. 5 Typical effect of Mach number on trim drag.

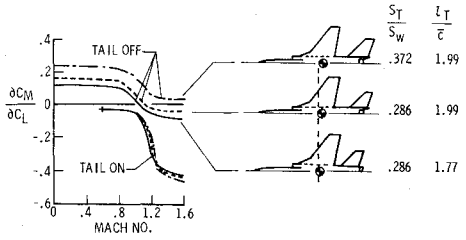

Fig. 6 Calculated effect of tail volume on stability level.

istics as a function of tail load is shown in Fig. 5 for Mach numbers of 0.90 and 1.60 at a typical maneuvering lift coefficient appropriate to each Mach number. The difference in the curves is primarily due to Mach number effects on the wing-body drag due to lift and downwash.

Supersonic aircraft typically trim with slight uploads at subsonic speeds as is illustrated by the symbol on the solid curve. The aerodynamic center shifts aft with increasing Mach number as is illustrated by the insert of aerodynamic center (ac) vs Mach number and a down tail load is generally required for trim at the supersonic Mach number, which results in high trim drag. The magnitude of the down load on the tail can be reduced at supersonic speeds by the effective use of camber and twist to provide positive moment at zero lift and wing design procedures to minimize wing-body aerodynamic center shift with Mach number. Once these wing design effects have been optimized, further benefits in supersonic trim drag can be obtained by increasing the tail contribution to stability at subsonic Mach numbers. This effect moves both symbol points on Fig. 5 to the right and results in reduced trim drag at both subsonic and supersonic Mach numbers.

A calculated effect of increasing tail contribution to stability is shown in Fig. 6. The tail volume was varied by increasing the tail arm and size, as indicated by the sketches on Fig. 6. The center of gravity of the configurations was selected to give a total stability level of -0.03 at a Mach number of 0.60 for all configurations. A preliminary verification of the feasibility of the center-of-gravity selection was obtained with weight and balance calculations. The increase in stability contribution of the tail is shown as a function of Mach number by a comparison of the tail-off curves for the three configurations. The increase in tail volume in going from the configuration with the smallest tail volume (lower sketch) to the configuration with the largest tail volume (upper sketch) was sufficient to make the wing body unstable at a Mach number of 1.6. This unstable wing-body moment requires an uptail load for trim.

The calculated effect of the increase in tail volume on the total trimmed drag due to lift at a Mach number of 1.60 is shown on Fig. 7. As the tail volume is increased (from top sketch to bottom sketch), the trimmed drag due to lift is significantly reduced. The drag reduction at $C_L = 0.4$ is

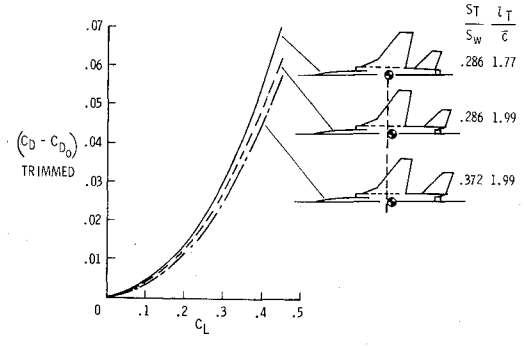

Fig. 7 Calculated effect of tail volume on trimmed drag-due-to-lift at $M = 1.6$; sharp-flat wing.

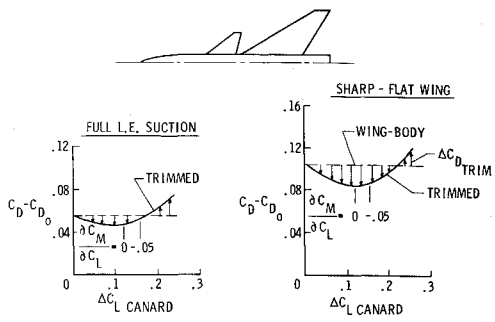

Fig. 8 Calculated effect of wing-body drag-due-to-lift on subsonic trim drag for canard configuration; $M = 0.70$; $C_L = 0.60$.

approximately 0.011. It should be noted that the calculated effect of this increase in tail volume on wave drag was approximately 0.001.

Canard Configurations

The discussion presented in the preceding sections of this paper has indicated the desirability of trimming an airplane with a positive load when the wing efficiency is low. The canard is, of course, an obvious way of achieving a positive load. Over the years, there has been interest in canard configurations for a number of reasons. The most noteworthy recent consideration of the canard is the trimmed high-lift capability obtained by Swedish researchers in the development of the Viggen aircraft.[6]

Recent unpublished theoretical studies by R. V. Harris Jr., of the NASA Langley Research Center have indicated that close-coupled canard configurations may have potential advantages as high-performance maneuvering aircraft in the low supersonic speed range. One specific potential advantage is reduction in wave drag compared to aft-tail configurations.

A computed variation of trimmed drag due to lift with canard trim load is presented in Fig. 8 for a close-coupled canard configuration. This figure, as in the section on the aft-tail configuration, is presented for wing-body drag-due-to-lift levels corresponding to full leading-edge suction and zero leading-edge suction as an illustration of the effects of drag due to lift on trim drag. Stability levels of 0 and -0.05 are indicated on the trimmed curve. The comments on wing-body drag due to lift made earlier with regard to Fig. 3 are, of course, equally valid for canard configurations.

For the sharp-flat wing case (zero leading-edge suction) the calculations indicate that trimming with a canard has a relatively large potential for reducing trim drag at low levels of stability. This would be expected, since for the conditions of zero leading-edge suction on the wing angle-of-attack effects are extremely important on the drag due to lift. Therefore, reducing the wing angle of attack by carrying part of the lift on the canard is beneficial, as was the case for the aft tail. When full leading-edge suction is developed on the wing, the advantage of carrying a large lift load on the canard is diminished. Consequently, as drag-due-to-lift improvements on the wing are made at the high-lift coefficients of interest for maneuvering, the advantages shown for the sharp-flat wing case (zero leading-edge suction) will be reduced.

The remainder of the discussion on canard configurations will be concerned only with the sharp-flat wing case (near-zero leading-edge suction), which is applicable to current wing drag-due-to-lift characteristics at the high-lift coefficients. For these wings, the trim drag is directly related to the wing drag due to lift which is approximately $C_D = C_L \cdot \tan\alpha$. Therefore, the ability to calculate the wing-body lift curve in the canard downwash field is of prime importance. Consequently, the following section is devoted to an assess-

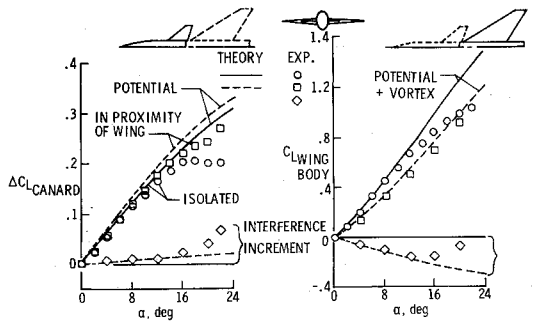

Fig. 9 Effect ot canard-wing interference for high sweep configuration; sharp-flat wing; $M = 0.70$.

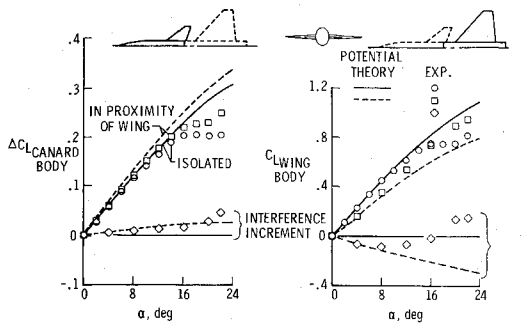

Fig. 10 Effect of canard wing interference for low sweep configuration; sharp-flat wing; $M = 0.70$.

ment of the applicability of existing theories to the prediction of subsonic canard-wing interference effects.

Use of Existing Theory for Prediction of Subsonic Interference Effects

A comparison of the experimental lift with theory is presented in Fig. 9 for the wing body, both isolated and in proximity to the canard body (right side of Fig. 9); and the canard body, isolated and in proximity to the wing-body (left side of Fig. 9). For this comparison, the wing and canard are coplanar. The canard had a leading-edge sweep of 52° and the wing leading edge was swept 60°.

The lift curves for the wing body were predicted using Ref. 3 in conjunction with the vortex-lift theory developed by Polhamus.[7] The theory agrees well with experiment for the isolated wing body up to an angle of attack of about 12° where the vortex flow begins to break down, as would be expected from the boundaries presented in Ref. 8. The significant point is that the vortex lattice theory gives a good prediction of the interference of the canard downwash on the wing as is indicated by the agreement of theory and experiment for the wing in proximity to the canard. Therefore, the lift curve for the wing body in proximity to the canard is reasonably well predicted by the theory up to about 20° angle of attack. A comparison of the interference lift increment obtained by experiment and theory is shown on the lower part of the figure and good agreement is noted up to an angle of attack of about 12°, which corresponds to the point of vortex breakdown on the isolated wing body.

Theoretical predictions of the canard-body lift were made using only the potential lift term of Ref. 7 with the constant in the equation being determined from Ref. 3. These results are compared with the experimental lift on the left of Fig. 9. The canard-body lift coefficient is based on the wing reference area, and the difference in lift coefficient scale from the wing characteristics should be noted. The theory overpredicts the lift for both the isolated canard body and the canard body in proximity to the wing. This discrepancy is not fully understood, but is presumed to be associated with fuselage interference effects.

The increase in canard-body lift due to upwash generated ahead of the wing, shown plotted at the bottom of the figure as an interference increment, is reasonably well predicted by theory at angles of attack to about 16°. At the angles of attack greater than 16°, the favorable interference is greater than the theory predicts.

The mutual beneficial interference between canards and wings at high angles of attack has been recognized for some time, and the area has been extensively reported in Ref. 6. This research utilized highly swept delta canards on which fully developed vortex flow existed as opposed to the lower sweep, higher aspect ratio canards of this investigation.

The calculated and experimental lift for a canard configuration having a wing leading-edge sweep of 44° is presented in Fig. 10. In this case, only the potential lift term of Ref. 7 was considered for both the canard and wing due to the low sweep angles. The comparison of the theoretical and experimental lift for the canard body (left side of the figure) shows generally the same trend as discussed previously. The isolated wing-body lift (right side of the figure) is reasonably well predicted up to about 12–14° angle of attack. In the case of the wing body in proximity to the canard, the calculated lift curve agrees with experiment in the low angle-of-attack range ($\alpha \leq 4°$). At angles of attack greater than about 8°; the interference of the canard results in significantly higher lift on the wing than the theory predicts and delays wing stall. A completely satisfactory explanation for this effect has not been demonstrated. It is interesting to note that although achievement of full vortex lift at this wing sweep would not be expected, as pointed out earlier, the wing lift in the presence of the canard approaches the value predicted by the theory with full vortex lift included (see Fig. 11). It must be recognized, however, that this favorable interference may be associated with some phenomenon other than a favorable effect of the canard on the wing vortex characteristics and that the agreement shown in Fig. 11 may be fortuitous.

The comparisons of theory and experiment that have been presented are for configurations where the wing and canard are coplanar, as indicated earlier in the discussion. The desirability of locating the canard above the wing chord plane has been shown by past research.[6] However, the mathematical model used in the present study to compute the canard-wing interference can only handle the coplanar case satisfactorily at this time.

Figure 12 shows a comparison of experimental data for a high canard configuration with a coplanar calculation. The lift curves for the canard body and the wing body in proximity to each other are reasonably well predicted up to about 16° angle of attack.

With the foregoing as validation, the coplanar calculations of canard-wing interference were used in an assessment of canard configuration trim drag characteristics at subsonic speeds.

Canard Configuration Trim Drag

The calculated trim drag is compared with experiment in Fig. 13. The comparisons are shown for lift coefficients of

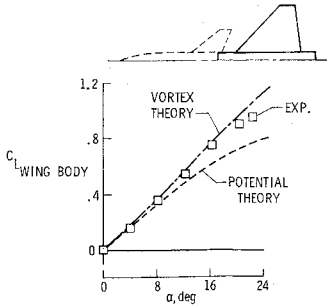

Fig. 11 Comparison of vortex-lift theory with experiment for low sweep wing in proximity to canard; $M = 0.70$.

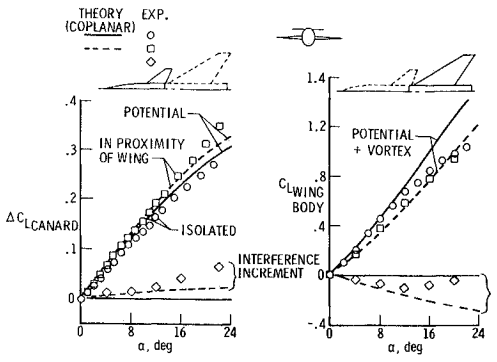

Fig. 12 Comparison of co-planar theory with experiment for high canard; sharp-flat wing; $M = 0.70$.

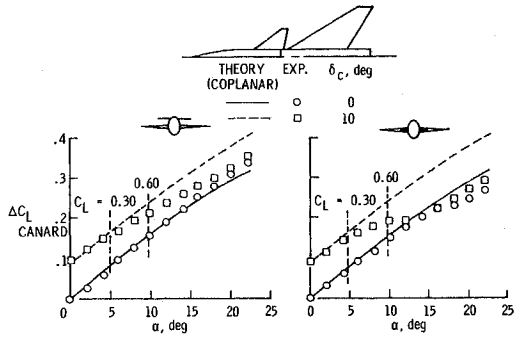

Fig. 14 Effect of canard height on control effectiveness; sharp-flat wing; $M = 0.70$.

0.3 and 0.6 at Mach number of 0.7. The solid symbols and tick on the calculated curve represent trim points at 5% static margin. The agreement between the calculated and experimental trim drag is reasonably good at the low-lift coefficient with a small effect of canard height indicated. At a lift coefficient of 0.6, the experimental trim drag is significantly higher than predicted by the calculations with the coplanar configuration exhibiting about 360 drag counts higher trim drag than the high canard configuration at 5% static margin.

The high trim drag shown by the experimental data in this case is the result of canard stall at the deflections required for trim. This is illustrated in Fig. 14 where the canard lift at 0° and 10° canard incidence is shown for the high canard and the canard in the wing chord plane. The angles of attack at which total lift coefficients of 0.30 and 0.60 occur are also indicated for reference. The high canard at 10° deflection shows a slight loss in effectiveness at $\alpha \approx 5°$ ($C_L = 0.3$), and at $\alpha \approx 10°$ ($C_L = 0.60$) the canard lift due to incidence is only about 75% of the zero angle-of-attack value. The canard in the wing chord plane shows a slightly greater loss in control effectiveness at $\alpha \approx 5°$ ($C_L = 0.30$) than the high canard. At the higher angle of attack ($\alpha \approx 10°$), the chord plane canard maintains only about 40% of the effectiveness shown at zero angle of attack.

The data of Fig. 14 bring to light one of the problems facing the designer of a close-coupled canard configuration as a highly maneuverable aircraft, that is, the task of providing an optimum method of longitudinal trim control. If trim is obtained through changing incidence of the canard, this would seem to dictate a more highly swept canard configuration to alleviate canard stall at high angles of attack. Such configurations, unfortunately, tend to have high drag-due-to-lift characteristics and would be expected to exhibit high trim drag. The use of trailing-edge flaps or elevons on the canard and/or wing offer a reasonable possibility in the subsonic speed range, but at supersonic speeds these types of control are not noted for either their control power capability or low trim drag characteristics. The concept of balancing the aircraft so that it is unstable at subsonic speeds and using an augmentation system for stability is, of course, an interesting

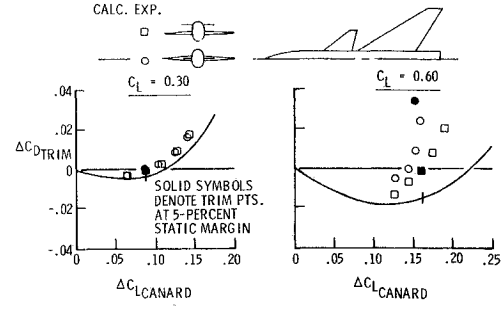

Fig. 13 Effect of lift coefficient on subsonic trim drag for canard configuration; sharp-flat wing; $M = 0.70$.

possibility. However, it must be kept in mind that this would tend to keep the canard operating at low angles of attack and would be expected to destroy some of the favorable mutual interference effects exhibited by close-coupled canard-wing configurations. Additional research effort is required before these equations can be answered adequately.

One of the objectives of this continuing study is to compare the trimmed drag due to lift of canard and aft-tail configurations. Aircraft employing aft tails for longitudinal stability and control have been in service for many years and the basic design problems encountered and the applicability of existing theories to these design problems are generally understood. Our research efforts on close-coupled canard configurations, however, have not been as extensive. Consequently, the design problems associated with canard configurations such as optimizing the mutually beneficial interference effects between a close-coupled canard and wing, while providing optimum longitudinal control from drag considerations, are not so well understood. Also, the applicability of existing theories for predicting the interference effects of close-coupled canard-wing configurations has not been documented over the Mach number range. Therefore, a completely valid comparison between optimized aft-tail and canard configurations cannot be made at this time.

Conclusion

The results of a preliminary analytical and experimental study of trim drag characteristics at maneuvering lift coefficients have been summarized. The study included aft-tail configurations at subsonic and supersonic speeds and canard configurations at subsonic speeds.

It is shown that the tail load required to minimize trim drag is highly dependent on the wing-body drag-due-to-lift characteristics, with examples presented for both the full and zero leading-edge suction cases. For the high drag case (corresponding to zero leading-edge suction), which tends to be typical at high maneuvering lift coefficients and high speeds, rather large uploads on the tail are required to reduce the trim drag problem. The analytical predictions of trim drag characteristics compare well with the experiment for the aft-tail configuration. At supersonic speeds, reductions in down tail load required to trim, obtained by increasing tail volume and thereby allowing a favorable rebalancing of the aircraft, result in relatively large reductions in trim drag for aft-tail configurations.

The vortex lattice lifting surface theory gives good predictions of the subsonic mutual interference effects for close-coupled canard configurations at low and moderate angles of attack for the 60° swept wing. The low sweep wing (44.0° sweep of leading edge) of the investigation shows beneficial high lift effects of the canard on the wing that are not predicted by potential flow theory.

At subsonic speeds, the experimental studies for the canard configuration exhibit considerably higher trim drag than the analytical prediction as a result of canard stall. One of the

primary design problems for canard configurations is finding a suitable means of longitudinal trim control that alleviates the canard stall problem while maintaining the high angle-of-attack benefits associated with close-coupled canard wing configurations.

References

[1] Graham, M. E. and Ryan, B. M., "Trim Drag at Supersonic Speeds of Various Delta Planform Configurations," TN D-425, 1960, NASA.

[2] Norton, D. A., "Airplane Drag Prediction," *International Congress on Subsonic Aeronautics*, Nov. 22, 1968, pp. 306–328.

[3] Margason, R. J. and Lamar, J. E., "Vortex Lattice Fortran Program for Computing Subsonic Aerodynamic Characteristics of Complex Planforms," TN D-6142, Dec. 1970, NASA.

[4] Middleton, W. D. and Carlson, H. W., "Numerical Methods of Estimating and Optimizing Supersonic Aerodynamic Characteristics of Arbitrary Planform Wings," *Journal of Aircraft*, Vol. 2, No. 4, July-Aug. 1965, pp. 261–265.

[5] Henderson, W. P., "Studies of Various Factors Affecting Drag-Due-to-Lift at Subsonic Speeds," TN D-3584, 1966, NASA.

[6] Behrbohm, H., "Basic Low-Speed Aerodynamics of Short-Coupled Canard Configurations of Small Aspect Ratio," TN 60, July 1966, SAAB.

[7] Polhamus, E. C., "A Concept of the Vortex Lift of Sharp-Edge Delta Wings Based on a Leading-Edge Suction Analogy," TN D-3767, 1966, NASA.

[8] Polhamus, E. C., "Predictions of Vortex-Lift Characteristics Based on a Leading-Edge Suction Analogy," *Journal of Aircraft*, Vol. 8, No. 4, April 1971, pp. 193–199.

AUGUST 1971 J. AIRCRAFT VOL. 8, NO. 8

Parameter Variation—An Insight to V/STOL Design

ARTHUR G. JONES*

Air Force Flight Dynamics Laboratory, Wright-Patterson Air Force Base, Ohio

Dimensional stability derivatives gathered from a simulator during the development of the XV-4B aircraft have been varied one and two at a time in a computer program for extracting the roots of the lateral-directional characteristic equation. These roots have been used to provide complex plane plots indicating the effect of derivative variation on the dynamic characteristics of the vehicle. Secondary plots have been used to show the breakdown of the elements making up each derivative. The sources for these elements and factors affecting their prediction have been examined, along with changes required to modify the vehicle's dynamic characteristics. Some comparisons are made with other vehicles.

Nomenclature

C-rpm	=	cruise engines (2) % rev/min (diverted downward for lift)
CG%mac	=	center of gravity % wing mean chord
g	=	acceleration due to gravity, ft/sec^2
I_x, I_z	=	moment of inertia about the x and z stability axes
I_{xz}	=	product of inertia about stability axes
L	=	rolling moment, ft-lb, positive right wing down
L-rpm	=	lift engines (4) % rev/min
L_p, L_r, L_v	=	stability derivatives, rate of change of rolling moment divided by I_x with variable indicated by subscript
m	=	mass of aircraft (w/g) slugs
N	=	yawing moment, ft-lb, positive nose right
N_p, N_r, N_v	=	stability derivatives, rate of change of yawing moment divided by I_z with variable indicated by subscript
w	=	weight of aircraft lb
y	=	side force, lb, positive out right wing
Y_p, Y_r, Y_v	=	stability derivatives, rate of change of side force divided by mass with variable indicated by subscript
α	=	angle of attack, trim value equal to zero
γ_v	=	nozzle deflection (average of 6 engines) measured from a 10° aft position
δ_e	=	elevator position, positive trailing edge down
δ_f	=	flap deflection
θ	=	pitch attitude, positive nose up, trim value equal to zero
σ	=	real part of characteristic root,/sec
$j\omega$	=	imaginary part of characteristic root,/sec

Subscripts

p	=	perturbation rolling velocity, stability axes, positive for right wing down aircraft motion, rad/sec
r	=	perturbation yawing velocity, stability axes, positive for aircraft nose right motion rad/sec
v	=	perturbation side velocity, stability axes, positive for aircraft motion to the right

Presented as Paper 70-551 at the AIAA Atmospheric Flight Mechanics Conference, Tullahoma, Tenn., May 13–15, 1970; submitted June 5, 1970; revision received December 7, 1970.

* Aerospace Engineer.

I. Introduction

MANY tunnel tests are run and elaborate calculations made to predict aircraft stability characteristics, particularly in the development of V/STOL aircraft. However, there is always a question as to the accuracy of these predicted characteristics.

In recent years there has been an attempt to correlate various wind tunnel, calculated and flight test data to achieve a better understanding of what is required for more accurate predictions.[3,5–7] This work has been partially successful but more is needed. Here attention has been directed to examining the effect of varying values of stability derivatives to determine their effects on vehicle dynamic characteristics.

II. Approach

Five of what are considered the more important lateral-directional derivatives are examined relative to the dynamics of the XV-4B (Fig. 1).[2,4] These derivatives listed in the order of their effect on the dutch roll mode of the aircraft are L_v, N_v, L_p, Y_v, and N_r. All the nominal lateral-directional stability axis derivatives and trim conditions used for this paper are listed in Table 1.